Coherent Rayleigh Scattering

Jay H. Grinstead[1] and Peter F. Barker[2]

[1]*Optical Technology Division, National Institute of Standards and Technology, Gaithersburg, Maryland 20899*
[2]*Department of Mechanical and Aerospace Engineering, Princeton University, Princeton, New Jersey 08544*

(Received 21 January 2000)

The spectrum of coherent scattering induced by electrostriction in gases has been analyzed in the previously unexplored, free-molecule limit by solving Boltzmann's equation with a periodic force due to the optical fields. Calculated and measured spectra of several gases at rarefied conditions are nearly Gaussian with widths approximately 10% wider than the spontaneous Rayleigh widths. Our results are the first spectrally resolved measurements of coherent Rayleigh scattering in the free-molecule limit, where the hydrodynamic analysis of stimulated Rayleigh-Brillouin scattering does not apply.

PACS numbers: 42.65.Hw, 42.50.Vk, 47.45.Dt

Stimulated Rayleigh and Brillouin scattering, two non-resonant, nonlinear optical effects in gases and liquids induced by electrostriction, have been extensively studied for conditions in which the fluid can be described as a continuum. The density perturbation that occurs in response to the optical fields takes the forms of traveling acoustic waves (Brillouin scattering) and stationary isobaric density fluctuations (Rayleigh scattering). In the frequency domain, the spectral distribution and gain dynamics of these nonlinear processes have been analyzed using the linearized equations of hydrodynamics and the coupled-wave theory of nonlinear optics [1]. For rarefied gases, however, the mean-free path may be comparable to the length scale of the electrostrictive force gradients. The response of the gas to the driving force, and the spectrum of stimulated scattering, cannot adequately be described with the hydrodynamic solution.

In this Letter we analyze stimulated scattering at gas densities sufficiently low that microscopic motion must be considered. The polarization-decoupled, nearly degenerate four-wave mixing configuration of our experiment permits the spectrum of Bragg-diffracted light to be measured independently of the optical fields that induce the perturbation. The configuration is similar to the Brillouin-enhanced four-wave mixing process used for amplified phase conjugation [2]. In the low-density regime of the present experiment, the density perturbation results from a distortion of the local velocity distribution sustained by the traveling-wave electrostrictive force. This variation of nonresonant four-wave mixing is the coherent analog of spontaneous Rayleigh scattering at rarefied conditions because the width of the four-wave mixing spectral profile is in direct proportion to the width to the microscopic velocity distribution. However, the coherence of the optically induced density perturbation leads to a spectral distribution distinct from that of spontaneous Rayleigh scattering, which arises from statistically correlated microscopic density fluctuations. Stimulated Rayleigh-Brillouin gain spectroscopy in gases has been reported [3], but an analysis of the

coherent nature of the electrostrictive force interaction was neglected. Here we show that the optically induced density perturbation in the free-molecule limit can be characterized from a solution to Boltzmann's equation with a traveling-wave electrostrictive force as the driving term, and that spectra of coherent scattering computed with this solution show excellent agreement with measured spectra of several gases at rarefied conditions.

The coherent Rayleigh scattering process is shown schematically in Fig. 1. The two pump waves, E_1 and E_2, create a density perturbation due to the electrostrictive force acting on the molecules, and the probe wave E_3 Bragg diffracts off the perturbation to generate the signal wave E_4. The density perturbation $\Delta\tilde{\rho}$ induced by the two pump beams is a traveling wave that oscillates at the beat frequency of the pump waves, $\Omega = \omega_1 - \omega_2$, with grating wave vector $\mathbf{q} = \mathbf{k}_1 - \mathbf{k}_2$. Phase matching requires that the signal beam have frequency $\omega_4 = \omega_3 - \Omega$ and wave number $\mathbf{k}_4 = \mathbf{k}_3 - \mathbf{q}$. Following Boyd [1], tildes denote time-varying quantities, and their absence indicates amplitude.

The electric field of the interfering pump waves generates a periodic force normal to the wave fronts which acts on the molecules through an induced dipole moment. Ignoring the tensor nature of the polarizability α, the force per molecule at the beat frequency of the two pump beams is given by [4]
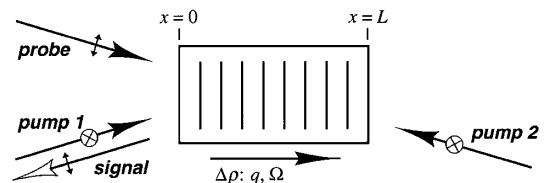
FIG. 1. Coherent Rayleigh scattering. The two pump waves create a traveling-wave density perturbation, and the phase-matched probe wave scatters off this perturbation to create the signal wave. The pump beams are orthogonally polarized to the probe and signal beams.

$$F = \frac{\alpha}{2} \frac{d}{dx} (\tilde{E}_1 + \tilde{E}_2)^2 = -\alpha q |A_1 A_2| \sin(qx - \Omega t),$$

$$(1)$$

where $q = |\mathbf{q}|$, A_1 and A_2 are the electric field amplitudes of the pump waves, and the direction x is parallel to the vector $\mathbf{q}$. An arbitrary phase factor has been neglected. It is assumed that amplitudes and phases of the pump waves remain constant through the interaction region. For a nonzero Ω, the periodic force becomes a traveling wave with velocity Ω/q. The periodic force imparts an acceleration to the molecules which distorts the x component of the local velocity distribution. The non-equilibrium velocity distribution leads to a spatially periodic density perturbation due to transport. In the hydrodynamic limit, the velocity distortion relaxes in a time short compared to the laser pulse duration, thus restricting individual particle displacement but causing bulk compression and rarefaction of the fluid. The usual conservation equations for mass, momentum, and energy adequately describe the dynamic response of the density perturbation under steady-state [1] and transient conditions [5]. In the free-molecule limit, however, the absence of equilibrating collisions precludes the transport of momentum and energy through viscous shear and heat conduction, respectively. The induced changes in particle trajectories from free flight result in a nonzero flux of particles through planes normal to the grating vector which, in turn, perturbs the local density. By simply accounting for particle motion statistically with a velocity distribution function, the density perturbation along the grating can be quantified.

The local velocity distribution can be considered to be a small departure f' from the equilibrium distribution f_0 under the influence of the induced force. As the force acts only on the x component of the velocity v, we assume that the velocity perturbation of the transverse components, which would arise only from direction-changing collisions with the nonequilibrium v distribution, can be neglected relative to the perturbation in v. The problem can then be reduced to one dimension, i.e., $f' = f'(x, v, t)$. The evolution of f' can be described by a one-dimensional Boltzmann equation:

$$\frac{\partial f'}{\partial t} + v \frac{\partial f'}{\partial x} + \frac{F}{m} \frac{\partial}{\partial v} (f_0 + f') = \left[\frac{\delta f}{\delta t}\right]_{\text{coll}}. \quad (2)$$

Here m is the molecular mass, f_0 is the normalized one-dimensional Maxwell distribution function, and $[\delta f/\delta t]_{\text{coll}}$ is the collision integral. If $\alpha |A_1 A_2| \ll k_B T$, where k_B is Boltzmann's constant and T is the gas temperature, the perturbation in the particle velocity due to the electrostrictive force is small relative to the average thermal velocity. This implies that f' is small relative to f_0 and that, to first order, $\partial f'/\partial v$ may be neglected relative to $\partial f_0/\partial v$. As we are interested in the response at sufficiently low densities where the time between collisions is long compared to the pump pulse duration,

the collision integral of Eq. (2) can be set to zero, yielding the collisionless Boltzmann, or Vlasov, equation. With these assumptions, Eq. (2) can be solved as an initial value problem with a zero initial condition, $f'(x, v, 0) = 0$:

$$f'(x, v, t) = \frac{\alpha |A_1 A_2|}{k_B T} f_0(v, \sqrt{2k_B T/m})$$

$$\times \frac{qv[\cos(qx - \Omega t) - \cos(qx - qvt)]}{qv - \Omega}.$$

$$(3)$$

The perturbation is linear in the amplitude of the forcing term and has a resonance at $\Omega = qv$, at which the traveling wave velocity matches the particle velocity. Particles moving with velocities at or near that of the traveling wave experience a force that is constant in phase, while particles moving at velocities different than the traveling wave are subject to a force that oscillates in direction.

The density perturbation is computed as $\Delta\tilde{\rho}/\rho_0 = \int_{-\infty}^{\infty} f' \, dv$, where ρ_0 is the equilibrium density. Integration of Eq. (3) over v is not possible in closed form, but the result can be written as

$$\frac{\Delta\tilde{\rho}}{\rho_0} = \frac{\alpha |A_1 A_2|}{k_B T} [g(\Omega/s) e^{i(qx - \Omega t)} + \text{c.c.}]. \quad (4)$$

The dependence of the perturbation amplitude on the traveling-wave velocity resides in g, a dimensionless complex-valued function of Ω normalized by a width parameter $s = q\sqrt{2k_B T/m}$. The function f' remains oscillatory in v with a frequency that increases with t, but the amplitude of its integral (i.e., g) asymptotes to a constant at $t \cong \pi/s$, which is approximately one-half the transit time across a fringe distance for particles moving with the most probable velocity. This time is the induction time of the electrostrictive perturbation and is fast compared to the laser pulse duration but slow compared to the induction time of Raman or electronic nonlinearities.

The electric-field amplitude A_4 of the four-wave mixing signal can be determined from the coupled-wave theory of nonlinear optics under the slowly varying envelope approximation [1] with the change in susceptibility being proportional to $\Delta\tilde{\rho}$. The steady-state intensity of the signal $I_4 \propto A_4 A_4^*$ in the small-signal limit over an interaction length L is

$$I_4 \propto (\alpha^2 L \omega_4 N/k_B T)^2 |g(\Omega/s)|^2 I_1 I_2 I_3, \quad (5)$$

where N is the particle number density and the I_i are the intensities of the three input beams.

The spectrum of the coherent signal is proportional to $|g|^2$ and, from numerical integration of Eq. (3), was found to be nearly Gaussian with a width approximately 10% wider than the Gaussian spectrum of spontaneous Rayleigh scattering. The slight departure from Gaussian behavior occurs in the wings (high traveling-wave velocities), where the value of the equilibrium distribution becomes negligible. The significant contribution to the integral of f'

in this non-Gaussian region arises from velocity groups near the center of the distribution, far from the traveling-wave velocity. The important result of the analysis is that, for a fixed scattering geometry, the width of the intensity spectrum depends on $\sqrt{T/m}$, which is identical to that of spontaneous Rayleigh scattering. However, the coherent spectral profile is unambiguously different owing to the interaction of the traveling-wave force with the entire velocity distribution at all points along the grating.

An experiment was designed to measure the spectral profile of the coherent Rayleigh scattering signal with sufficient resolution for comparison with theory. The required range of frequency detuning (Ω) between the pump beams was achieved through the use of a single broad band pump source. Interference between the two pump beams produces simultaneously all values of Ω within the laser bandwidth. A narrow band probe laser samples all the density gratings produced by the pump beams, and the signal consists of all phased-matched frequencies the four-wave mixing process can support. The frequency spectrum was resolved using an etalon and was recorded by monitoring the transmission of the signal beam as the probe laser frequency was scanned.

Two frequency-doubled, pulsed Nd:YAG lasers were used in this experiment. The pump and probe lasers were multimode and injection seeded, respectively. The cw injection-seed laser for the pulsed probe laser host could be temperature tuned in the fundamental (1.06 μm) over approximately 9 GHz with an external voltage ramp. A small portion of the seed laser was directed through a 250 MHz confocal reference cavity, which was locked to a frequency-stabilized HeNe laser. As the seed laser was scanned transmission through this reference cavity was used to monitor the scanning linearity and provide an accurate frequency calibration of the measured spectra.

The unseeded pump laser beam was split with a 50-50 beam splitter, and the two beams were crossed in a gas cell at an approximately 178° angle. The propagation distances from the beam splitter to the crossing point were matched to within a few mm. The pump laser bandwidth was approximately 40 GHz, and the distribution of Ω was estimated to be uniform within 5% over ±7 GHz. Both pump beams were polarized normal to the plane defined by their intersection. The probe beam was orthogonally polarized to that of the pumps and was counterpropagated against one of the pump beams (Fig. 1). All beams were focused to a diameter of approximately 100 μm, and the beam waists were coincident at the crossing point. The interaction length (L) was estimated at 1.5 cm based on the diameter and crossing angle of the beams. The two laser pulses (7 ns FWHM) were coincident in time with an estimated jitter of less than 2 ns. The generated four-wave mixing signal, which has the same polarization as the probe, counterpropagates against the other pump beam. After passing through the pump beam focusing lens, the

signal was coupled out through a thin-film polarizer and directed to the detection system approximately 7 m away.

The etalon used to characterize the spectrum was a temperature-stabilized 5 mm quartz flat (free spectral range 20 GHz) with a finesse of approximately 75. A portion of the probe beam was used to align the etalon and measure its transmission profile. The signal beam was then coupled on to this reference beam path with a polarizing beam splitter. Using appropriate beam splitters, four separate paths comprising both incident and transmitted reference and signal beams were created. The reference-beam intensities were measured with photodiodes, while the signal beams were measured with photomultiplier tubes. The transmission spectra of the reference and signal were normalized on a per-shot basis. Typically 50 pulses were averaged for each seed-laser frequency step. Drift of the etalon resonance relative to the calibrated probe laser frequency was assessed to be negligible from several consecutive weeks of use.

Shown in Fig. 2 is the measured transmission profile of the coherent Rayleigh scattering signal from N_2 at 298 K and 6.6 kPa (50 torr). The pulse energy of each of the input beams was approximately 15 mJ. No signal could be detected without the presence of all three input beams, indicating that the coherent signal at this pressure is at least an order of magnitude stronger than the spontaneous signal for the same geometrical collection efficiency ($f/30$). Also plotted in Fig. 2 is the transmission profile of the narrow band probe laser, which defined the resolution of the measurement. The mean-free path λ at this temperature and pressure is 1.3 μm assuming a hard-sphere collision diameter derived from the viscosity, which yields a Knudsen number (Kn $= \lambda q/2\pi$, ratio of mean-free path to
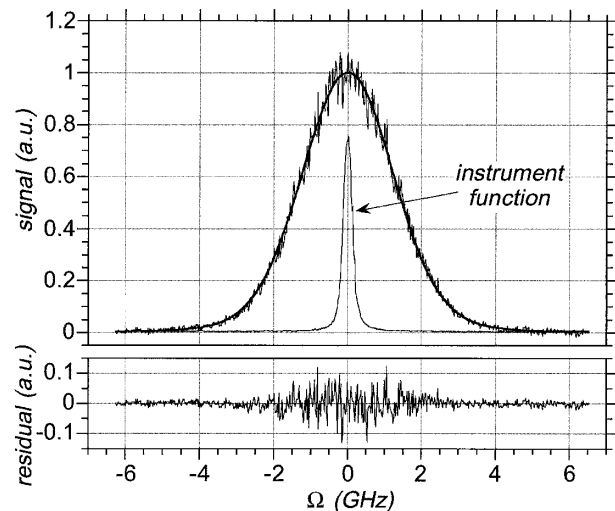
FIG. 2. Frequency spectrum of coherent Rayleigh scattering from N_2 at 6.6 kPa (50 torr) and 298 K. Instrument function is the transmission spectrum of the narrow band probe laser. The solid line is a curve fit of a numerical model to the data. The curve fit residual is shown below.

fringe spacing) of approximately 5. The tabulated average polarizability for N_2 [6] and the pump-pulse energies validate the small perturbation assumption: $\alpha|A_1A_2|/k_BT \approx 10^{-4}$. A curve fit of $|g(\Omega/s)|^2$ to the spectrum was performed and is plotted with the data. The curve-fit residual is shown below. Rather than attempt to deconvolve the instrument function from the data prior to curve fitting, $|g(\Omega/s)|^2$ was convolved with an analytic approximation to the instrument function as part of the fitting procedure. The width parameter s obtained from the curve fit agrees within 1% of the expected value based upon our q and T. The signal-to-noise ratio of the data in the wings, however, was insufficient to resolve the predicted non-Gaussian behavior. (For the pressure at which the spectrum was recorded, the mean time between collisions was approximately 6 ns, which is slightly shorter than the full widths of the laser pulses. Although some collisions will have occurred during the pulse, their frequency is sufficiently small as to not grossly invalidate the collisionless assumption.) The agreement between the calculation for the free-molecule limit (Kn $\gg$ 1) and the data is excellent. In the fully hydrodynamic limit, Kn $\ll$ 1 (i.e., liquids), the spectrum would exhibit Brillouin-shifted peaks due to the excited acoustic modes. The unshifted Rayleigh component would be homogeneously broadened, owing to the collective effects of collisions, with a width proportional to the thermal diffusion rate [1]. In the transition regime, which applies to gas densities for which Kn $\lesssim$ 3, the spectrum would exhibit both hydrodynamic and free-molecule behavior.

The fidelity of the calculation was further explored by measuring the coherent Rayleigh scattering spectra of CH_4, CO_2, and SO_2 at 298 K. The gas pressures were also 6.6 kPa with the exception of SO_2, which was 3.3 kPa (25 torr). At these conditions the Knudsen numbers and collision times were similar to that of N_2. The averages of s for each gas obtained from curve fits to several spectra are plotted in Fig. 3 as a function of molecular mass. The error bar for CH_4 denotes the expanded uncertainty with coverage factor $k = 2$ (i.e., 2 standard deviations); uncertainties for the other points are less than 1.7% and could not be shown legibly. The curve in Fig. 3 corresponds to the expected value of s as a function of molecular mass for our q and T. The agreement between the expected and measured widths for the three other gases is also excellent, confirming the predicted result that the coherent Rayleigh scattering spectrum is parametrized only by s.

We have presented a microscopic theory of coherent Rayleigh scattering induced by electrostriction in the free-molecule limit. This is in contrast to the previously documented analysis of stimulated Rayleigh-Brillouin scattering in the hydrodynamic limit, where the fluid is considered a continuum. The dynamic response of the optically induced density perturbation was characterized with a solution of a one-dimensional collisionless
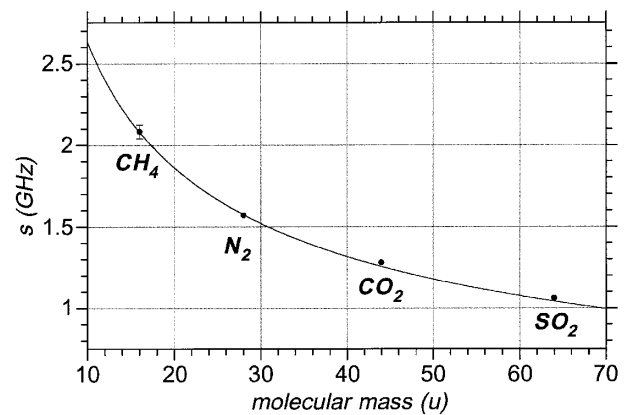
FIG. 3. Average of width parameter $s = q\sqrt{2k_BT/m}$ determined from curve fits to measured coherent Rayleigh scattering spectra of CH_4, N_2, CO_2, and SO_2 at 298 K as a function of molecular mass. The error bar for CH_4 denotes the expanded uncertainty with coverage factor $k = 2$ (i.e., 2 standard deviations); uncertainties for the other points are less than 1.7%. The curve corresponds to the predicted value of s for the experimental values of q and T.

Boltzmann equation in which the driving term is due to the traveling-wave electrostrictive force. The spectrum of Bragg-diffracted light is approximately Gaussian, in contrast to the Lorentzian profile predicted in the hydrodynamic limit. Excellent agreement between predicted and measured coherent Rayleigh scattering spectra was found for several gases under rarefied conditions. The technique provides a tremendous increase in sensitivity over spontaneous Rayleigh scattering while conveying the same information about the medium. Possible applications include validation of kinetic models of gases and gas mixtures, and translational temperature measurements in low to moderate density neutral and weakly ionized gases.

[1] R. W. Boyd, *Nonlinear Optics* (Academic Press, Boston, 1992), p. 355.
[2] W. A. Schroeder, M. J. Damzen, and M. H. R. Hutchinson, IEEE J. Quantum Electron. **25**, 460 (1989).
[3] C. Y. She, G. C. Herring, H. Moosmüller, and S. A. Lee, Phys. Rev. Lett. **51**, 1648 (1983); Phys. Rev. A **31**, 3733 (1985).
[4] Boyd, *Nonlinear Optics* (Ref. [1]), p. 327.
[5] W. Hubschmid, B. Hemmerling, and A. Stampanoni-Panariello, J. Opt. Soc. Am. B **12**, 1850 (1995).
[6] R. H. Orcutt and R. H. Cole, J. Chem. Phys. **46**, 697 (1967).